Ferromagnetism in tetragonally distorted chromium

Wuwei Feng, Dang Duc Dung, and Sunglae Cho*
Department of Physics, University of Ulsan, Ulsan 680-749, Republic of Korea
(Received 3 May 2010; revised manuscript received 5 July 2010; published 12 October 2010)

We report on the experimental observation of ferromagnetic ordering in the tetragonally distorted α phase of Cr, based on the anomalous Hall effect hysteresis and corroborated by magnetization hysteresis. The ferromagnetic ordering is reasonably ascribed to an increase in the out-of-plane lattice parameter of the α-Cr phase due to the low-dimensional connection to the δ-Cr crystal-lattice matrix, which suffers a large compressive lattice-mismatch strain from the substrate under two-dimensional growth. The low proportion of the α phase in the Cr film results in a weak macroscopic-scale ferromagnetic moment.

DOI: 10.1103/PhysRevB.82.132401 PACS number(s): 75.70.Ak, 75.50.Cc, 75.60.Ej

The 3*d* transition metals are of great importance to the study of magnetism and magnetic materials. Thin-film growth of these materials on semiconductor substrates has proven to be very important, both for potential applications and for fundamental research, due to the fact that thin films with reduced dimensions or altered structures grown on different substrates may exhibit magnetic properties very different from those of bulk materials. For example, bcc Co that does not occur in nature was obtained through epitaxial growth on a GaAs substrate.[1] To modify the lattice constant of a low-dimensional structure, the most common approach is to epitaxially stabilize a thin film on a suitable substrate. Unfortunately, the allowable modification of the lattice parameter is limited by the epitaxial strain relaxation and is rarely sufficient to form new magnetic phases. One interesting exception is that the antiferromagnet of bcc α-Mn could demonstrate ferromagnetic (FM) ordering when stabilized on a GaAs substrate.[2]

Cr is a 3*d* transition metal showing the unique spin-density wave antiferromagnetism with a small magnetic moment in the normally observed bulk form.[3] However, the very large moment ($\sim 5\ \mu_B$) in its atomic form suggests that peculiar magnetic effects might be observed in the low-dimensional Cr layers. The ferromagnetism of Cr has been predicted in metallic overlayers and interfaces[4] and in the hexagonal-closed-packed (hcp) structure[5] whereas previous theoretical calculations did not predict an occurrence of FM ordering in bcc Cr phase. Several groups attempted to prepare metastable Cr films on various substrates, including Ru (0001),[6] Cu (100),[7] Ag (100),[8] Pt (111),[9] Co (0001),[10] and GaAs (100).[11] However, apart from observation of a weak FM ordering in hcp chromium in Cr/Ru (0001) superlattices,[12] little information regarding the magnetic properties of Cr films was reported. In this Brief Report we report the observation of FM ordering in the tetragonally distorted α phase of Cr. Opening this work to public probably would stimulate renewed interests on bcc Cr in both theoretical and experimental studies.

Cr films with thickness of 50–100 nm were prepared in a standard solid-source molecular beam epitaxy (MBE) chamber (VG Semicon model V80). A 200-nm-thick GaSb buffer layer was first grown on Si (100) substrate at 560 °C. The Cr films were then deposited on GaSb buffer under an ultrahigh vacuum of 10^{-9} Torr, followed by the growth of ~9 nm GaSb cap to avoid the contamination of inner layers of Cr. Reflection high-energy electron diffraction (RHEED) was applied to monitor the growth process of the Cr films. The crystal structure and lattice constant were determined by x-ray diffraction (XRD) using Cu $K\alpha$ radiation. The magnetic properties were characterized by superconducting quantum interference device magnetometer (Quantum Design Inc.). A x-ray photoemission spectroscopy (XPS) depth-profile composition measurement was carried out to indicate the Cr/GaSb interface alloying effect. Hall measurement using a van der Pauw geometry was carried out to manifest the existence of anomalous Hall effect (AHE), which has historically been an important tool to study magnetization processes in ferromagnetic materials.[13] It is generally believed that the AHE hysteresis shown in the Hall measurement will be consistent with the magnetization hysteresis obtained in the magnetometry measurement.[14]

A high-quality epitaxial Sb-stabilized GaSb buffer layer with sharp (1×3) surface reconstruction is achieved as seen from Fig. 1(a), in agreement with the surface-reconstruction phase diagram for GaSb.[15] The Stranski-Krastanov growth mode is dominant when the Cr films are grown from room temperature to 200 °C, as shown in Fig. 1(b). The regular, symmetric distribution of spots in the RHEED pattern probably just results from the bcc structure of the film with the electron-beam azimuth along $[1\bar{1}0]$ direction of the GaSb(100) substrate and was not element dependent. Because we have also observed a very similar RHEED pattern in the 30 °C-grown Fe/GaSb(100) film (not shown), considering that Fe and Cr are both bcc structures and have similar lattice constants. The island tendency is almost suppressed when the Cr film is grown at 300 °C, with distinct streaky lines appearing over the entire Cr film growth, as shown in Fig. 1(c). When grown at 400 °C, the chevron-shaped spots shown in Fig. 1(d) might be attributed to the surface faceting

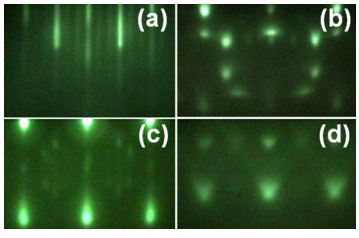

FIG. 1. (Color online) RHEED patterns for (a) the GaSb buffer and the Cr films grown at (b) 30–200 °C, (c) 300 °C, and (d) 400 °C.

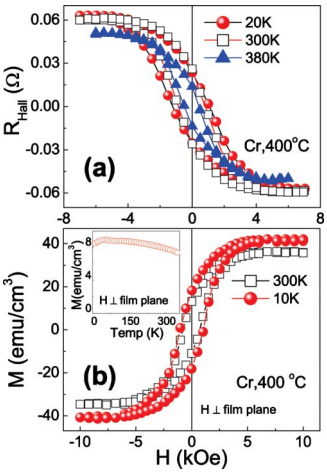

FIG. 2. (Color online) Magnetic field dependence of (a) the anomalous Hall resistance and (b) the magnetization hysteresis loops for the 100-nm-thick Cr film grown at 400 °C. The inset (b) shows the zero-field-cooling M-T curve under the applied field of 500 Oe.

on which fine particles with regular ridge-and-valley nanoscale structures were formed.[16,17]

Surprisingly, FM properties are observed in the 400 °C-grown Cr films based on the evident AHE hysteresis and magnetization hysteresis, as shown in Figs. 2(a) and 2(b). The magnetization moment is relatively weak while the Curie temperature is high as judged from the persistence of AHE hysteresis loop at 380 K. We repeated sample preparations and characterizations and confirmed the reproducibility of the interesting observation.

We began with the crystal structure analysis in order to shed light on the observed FM ordering in Cr film. Figure 3 shows the XRD spectra of the Cr films grown at temperatures ranging from 30 to 500 °C. By careful examination, we determined that bcc α-Cr coexists with A15-type δ-Cr having a primitive cubic structure at growth temperatures above 200 °C, in agreement with the coexistence of α and δ phases in the bulk or film Cr as ordinarily observed.[18–20] Both Cr phases can be epitaxially grown on GaSb (100). The α-Cr is the dominant phase at the lower growth temperature. However, δ-Cr grows to good crystallinity and progressively becomes the majority proportion with increasing growth temperature. Another phase of polycrystalline *ta*-Cr occurring when the Cr film is grown at or above 400 °C exhibits almost the same structure as that of δ-Cr but a different space group. The presence of regularly distributed *ta*-Cr fine particles is verified by the surface faceting observed in the RHEED pattern in Fig. 1(d). The most important characteristic in the XRD spectra is the notable shift of α-Cr (200) toward lower 2θ position for the Cr film grown at 400 °C, indicating a sufficient expansion of the out-of-plane lattice parameter ($a_\perp$), which might be the cause responsible for the observed FM properties.

FM property is not observed in the 500 °C-grown Cr film composed of δ- and *ta*-Cr phases according to the absence of AHE hysteresis in the Hall measurement. This can be explained by the disappearance of α phase in that Cr film and also indicates that δ-Cr and *ta*-Cr do not contribute to the

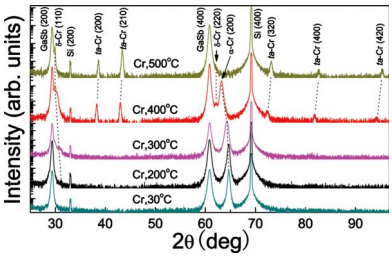

FIG. 3. (Color online) θ-2θ XRD patterns for the 100-nm-thick Cr/GaSb (100) films grown at temperatures ranging from 30 to 500 °C.

observed FM ordering. The M-T curve shown in the inset of Fig. 2(b) exhibits an increase in susceptibility below 80 K, which might be due to the antiferromagnetic ordering in δ-Cr at low temperature.

Matsuo *et al.*[21] have also observed a weak ferromagnetism in bcc Cr fine particles, which was ascribed to the surface magnetism due to the high density of states of electrons at the surface and the relative deficiency of nearest-neighbor atoms leading to energy-band narrowing. This scenario has been predicted and experimentally validated but was still under inconsistency.[22–24] In our case, the *ta*-Cr fine particles are embedded in the α- and δ-Cr epitaxial films, giving rise to a number of *ta*-Cr/epitaxial-Cr interfaces. However, the *ta*-Cr/epitaxial-Cr interface magnetism probably cannot contribute to the observed FM ordering due to the absence of FM ordering in the 500 °C-grown Cr film. In addition, we found that the Cr phase evolution can be somewhat different even when grown at the same temperature probably due to a slight deviation of tiny growth conditions, such as the cleanness of wafer surface and/or GaSb buffer quality, etc. We have also obtained a 400 °C-grown Cr sample exhibiting notable FM properties (not shown here), in which the *ta*-Cr XRD peaks are almost suppressed. Therefore, the *ta*-Cr phase probably has no direct connection with the observed FM properties. The coexistence of α and δ phases is ordinarily observed in previously reported bulk or thin-film Cr samples,[18–20] where no FM properties were observed. Therefore, it seems hard to believe that the interface ferromagnetism between α- and δ-Cr phases will be responsible for the observed FM property in our case.

The 200-nm-thick GaSb buffer is nonmagnetic according to Hall measurement. The Cr films were deposited under an ultrahigh vacuum of 10^{-9} Torr in the MBE chamber and the Cr raw material is of high purity of 99.99%. Therefore, Cr alloying with other impurities will not happen during the film growth of Cr layers. A XPS depth-profile composition measurement for the 400 °C-grown Cr film was carried out to study the interface alloying effect between Cr layers and GaSb buffer, as shown in Fig. 4. The atomic composition of Cr sharply increases to 100% at the depth of ~10 nm, where is the onset of Cr layers. We note that the penetration depth of XPS is ~10 nm. Therefore, the interface between GaSb cap and Cr layers is very sharp probably due to the deposition of cap layer at a decreased temperature (100–200 °C) after the growth of Cr layers is finished. The interdiffusion region between Cr layers and GaSb buffer seems thicker. However, the real interdiffusion region probably is within 10

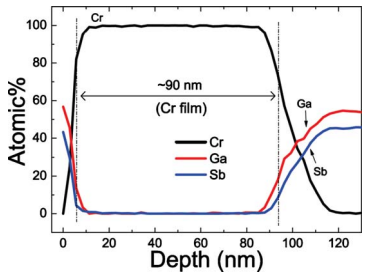

FIG. 4. (Color online) The XPS depth-profile measurement for the 100-nm-thick Cr film grown at 400 °C.

nm, considering the penetration depth of XPS. Therefore, we can safely conclude that at least ~90% of Cr layers in the 100-nm-thick Cr sample are pure Cr, where no alloying process occurs.

Those thin interface alloys possibly composed of Cr, Ga, and Sb elements cannot be the cause of the observed FM ordering in the Cr film. Because the interface alloying process will become more serious in the 500 °C-grown Cr sample, compared to the case grown at 400 °C. If the interface alloys play important role, ferromagnetism will probably become a common observation when the Cr films are grown at high temperatures and, of course, should also be observed in the 500 °C-grown Cr sample. However, we only observed FM properties in the 400 °C-grown Cr sample. Therefore, the alloying effect on the structural and magnetic properties of Cr film can be safely ruled out.

Figure 5 shows the XRD pattern and *M-H* data for another 400 °C-grown Cr film with a thickness of 50 nm. The α-Cr (200) peak position of this Cr sample is the same as that of 400 °C-grown Cr film shown in Fig. 3. The difference between these two Cr samples is that the content of α phase in the Cr sample shown in Fig. 5 is much smaller than that of the Cr sample shown in Fig. 3, as judged from the intensity of α-Cr (200) peak in two samples. As a result, the Cr sample shown in Fig. 5 demonstrates greatly reduced FM moment, several times smaller than that of the Cr sample shown in Fig. 3. Therefore, the reduced composition of α phase in the 400 °C-grown Cr film leads to a reduced FM

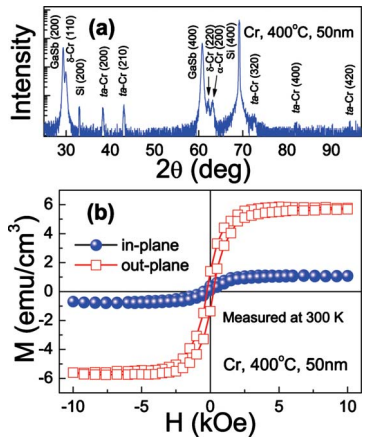

FIG. 5. (Color online) (a) θ-2θ XRD pattern and (b) the corresponding *M-H* data for another 400 °C-grown Cr film with the thickness of 50 nm.

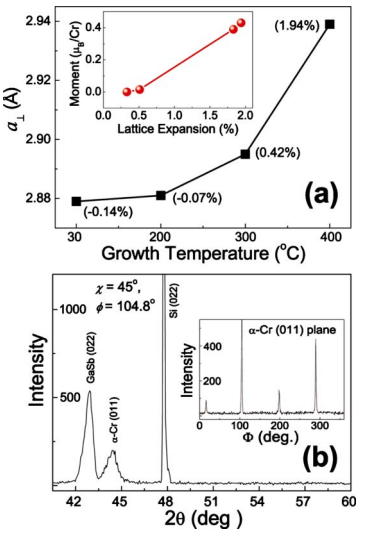

FIG. 6. (Color online) (a) The lattice constant ($a_\perp$) variation as a function of growth temperature for the α-Cr phase. The lattice constant ($a_\perp$) expansion ratio shown in the parentheses is calculated using $(a_\perp - a_{\text{bulk}})/a_{\text{bulk}}$, where $a_\perp$ is the Cr lattice parameter perpendicular to the film plane and the a_{bulk} is the bulk lattice parameter of bcc Cr. The inset shows the correlation between the lattice parameter ($a_\perp$) expansion and the magnetic moment per α-Cr atom. (b) The θ-2θ scan of α-Cr (011) in a skew geometry for the 400 °C-grown Cr film with a thickness of 100 nm. The inset shows the Φ scan of α-Cr (011).

moment, indicating that the observed FM properties come from the α-Cr phase at the expanded lattice parameter.

The volume composition of α-Cr phase is calculated as approximately 12% for the 400 °C-grown Cr film shown in Fig. 3 by comparing the integrated diffraction intensity of α-Cr (200), *ta*-Cr (200), and δ-Cr (110) according to the equation $I_{hkl}=I_0VF_{hkl}^2/v^2$, where I_0 is the intensity of incident beam, V is the volume of the crystal, v is the volume of unit cell, and F_{hkl} is the structure factor.[25] The magnetic moment per α-Cr atom is then calculated as 0.43 μ_B, considering that the net magnetic moment arises from α-Cr only. As shown in Fig. 6(a), the parameter ($a_\perp$) of α-Cr is at equilibrium state or only slightly enhanced when Cr films are grown at 300 °C or below and thus cannot induce ferromagnetism according to the Bethe-Slater curve. When grown at 400 °C, a larger expansion of 1.94% is observed, which triggers the ferromagnetism in the Cr film. In addition, we have also observed an increase in magnetic moment per α-Cr atom with increasing lattice parameter ($a_\perp$) expansion, as shown in the inset of Fig. 6(a), which is calculated from several selected Cr films. This is also a strong evidence to ascribe the observed FM ordering to the α-Cr phase at expanded structure.

Figure 6(b) shows the θ-2θ scan spectra for the α-Cr (011) in a skew geometry at one of the azimuthal positions. In skew configuration other crystallographic planes which are not parallel with the thin-film plane can be measured.[26] According to the θ-2θ scan data for the Cr (011) and (200) planes, the in-plane lattice parameter ($a_\parallel$) is determined to be 2.826 Å, smaller than that of bulk α-Cr. Therefore, the α phase in the 400 °C-grown Cr film is actually a tetragonally

distorted cubic with $a_{\parallel}=2.826$ Å and $a_{\perp}=2.941$ Å. The inset of Fig. 6(b) shows a Φ scan of the α-Cr (011) exhibiting fourfold symmetry, consistent with a cubic structure.

What is the mechanism responsible for the observed parameter ($a_{\perp}$) expansion? The primary contribution could not have been due to thermal strain, since the respective thermal-expansion coefficient at 300 K, 4.9×10^{-6} K^{-1} for Cr and 6.1×10^{-6} K^{-1} for GaSb, are comparable. We found that the choice of GaSb substrate is critical for the epitaxial stabilization of Cr films due to the fact that only polycrystalline Cr film can be obtained when grown on GaAs (100) or Si (100) substrates at 400 °C, which have smaller lattice constants than that of GaSb. The lattice mismatch with GaSb substrate for both Cr phases is within acceptable limits, as shown in Fig. 7(a), thus allowing for stabilization of them on GaSb (100).

It is noticed that the δ-Cr constitutes the majority of the phase in the 400 °C-grown Cr film. Although GaSb substrate exerts tensile strain on the α-Cr when α-Cr (100) is stabilized on GaSb (100) [see Fig. 7(a)], contrary to the observed reduction in $a_{\parallel}$, this contribution can be ignored due to the low proportion of the α phase. On the contrary, GaSb substrate exerts compressive strain on the dominant δ-Cr phase when δ-Cr (110) is stabilized on GaSb (100), as shown in Fig. 7(a). This significant lattice strain, assisted by an increase in thermal strain with increasing growth temperature, gives rise to the notable reduction in $a_{\parallel}$ and, therefore, the expansion of $a_{\perp}$ for the δ-Cr phase governed by an elastic strain picture. The minority of the α-Cr phase is two dimensionally connected to the δ-Cr crystal lattice and thus also suffered the compressive strain in the in-plane direction, inducing the observed expansion of $a_{\perp}$ of the α-Cr phase due to elastic strain picture, as shown Fig. 7(b). When Cr films are grown at low temperatures, the α-Cr constitutes the majority of the phase. Therefore, GaSb substrate exerts tensile strain on the Cr film as a whole, which results in the negligible $a_{\perp}$ expansion for the α-Cr phase, as shown in Fig. 7(c), explaining the absence of FM ordering in the Cr films grown at low temperatures.

A significant level of strain exists in the 400 °C-grown Cr film and, actually, can be directly observed on a macroscopic scale (not shown). When, after growth, the Cr sample is being removed from the substrate holder by loosening the bolts, the small perturbation from the bolts may have caused part of Cr film surface to crack due to the significant strain exists in the Cr film when it is two-dimensionally stabilized on GaSb (100).

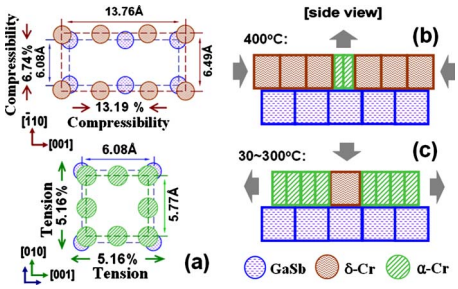

FIG. 7. (Color online) (a) Calculated lattice mismatch strain with GaSb (100) substrate for the nonreconstructed δ-Cr (110) and α-Cr (200). The schematic of lattice mismatch strain exerted on Cr film when grown at (b) 400 °C and (c) low temperatures.

The observation of ferromagnetism in the Cr film with thickness up to 100 nm is very unique because it is only observed when the Cr film is grown on GaSb (100) at 400 °C; no FM properties are observed when Cr films are grown on GaSb (100) at other temperatures; no FM properties are observed when Cr films are grown on other substrates, such as GaAs (100), Si (100), at different growth temperatures.

In summary, we grew epitaxially stabilized Cr thin films on GaSb (100) using the MBE technique. In films up to 100 nm in thickness, a weak FM ordering was experimentally observed. Although the contribution of interface ferromagnetism between α- and δ-Cr phases cannot be completely ruled out, this observation is reasonably ascribed to a significant lattice parameter expansion in the tetragonally distorted α-Cr phase. The results of this study could prove interesting and important in both forming a comprehensive understanding of chromium and the underlying physics.

This work was supported by the National Research Foundation of Korea (NRF) funded by the Ministry of Education, Science and Technology (Grant No. R0A-2006-000-10241-0) and Priority Research Centers Program (Grant No. 2009-0093818).

*Corresponding author; slcho@ulsan.ac.kr

[1] G. A. Prinz, Phys. Rev. Lett. **54**, 1051 (1985).
[2] Y. Hwang *et al.*, Phys. Rev. B **79**, 045309 (2009).
[3] E. Fawcett, Rev. Mod. Phys. **60**, 209 (1988).
[4] C. L. Fu *et al.*, Phys. Rev. Lett. **54**, 2700 (1985).
[5] D. A. Papaconstantopoulos *et al.*, Phys. Rev. B **39**, 2526 (1989).
[6] M. Albrecht *et al.*, Surf. Sci. **415**, 170 (1998).
[7] J. Jandeleit *et al.*, Surf. Sci. **319**, 287 (1994).
[8] D. Rouyer *et al.*, Surf. Sci. **331-333**, 957 (1995).
[9] L. Zhang *et al.*, Surf. Sci. **371**, 223 (1997).
[10] P. Ohresser *et al.*, Surf. Sci. **352-354**, 567 (1996).
[11] D. Qian *et al.*, J. Cryst. Growth **218**, 197 (2000).
[12] M. Albrecht *et al.*, Phys. Rev. Lett. **85**, 5344 (2000).
[13] C. L. Chien and C. R. Westgate, *Hall Effect and Its Applications* (Plenum, New York, 1980).
[14] R. Ramaneti *et al.*, Appl. Phys. Lett. **91**, 012502 (2007).
[15] A. S. Bracker *et al.*, J. Cryst. Growth **220**, 384 (2000).
[16] T. Hanada *et al.*, Phys. Rev. B **64**, 165307 (2001).
[17] A. Sugawara and K. Mae, Surf. Sci. **558**, 211 (2004).
[18] M. R. Fitzsimmons *et al.*, Phys. Rev. B **48**, 8245 (1993).
[19] L. Saraf *et al.*, Appl. Phys. Lett. **82**, 2230 (2003).
[20] K. Kimoto *et al.*, J. Phys. Soc. Jpn. **22**, 744 (1967).
[21] S. Matsuo *et al.*, J. Phys. Soc. Jpn. **44**, 1387 (1978).
[22] C. L. Fu and A. J. Freeman, Phys. Rev. B **33**, 1755 (1986).
[23] L. E. Klebanoff *et al.*, Phys. Rev. B **30**, 1048 (1984).
[24] D. R. Grempel, Phys. Rev. B **24**, 3928 (1981).
[25] C. G. Darwin, Philos. Mag. **27**, 315 (1914).
[26] V. M. Kaganer *et al.*, Phys. Rev. B **72**, 045423 (2005).